D-Mannose Binding, Aggregation Property, and Antifungal Activity of Amide Derivatives of Pradimicin A

Wataru Miyanishi,[a] Makoto Ojika,[a] Dai Akase,[b] Misako Aida,[c] Yasuhiro Igarashi,[d] Yukishige Ito,[e,f] Yu Nakagawa[a,f,g,*]

[a]*Department of Applied Biosciences, Graduate School of Bioagricultural Sciences, Nagoya University, Furo-cho, Chikusa-ku, Nagoya 464-8601, Japan*

[b]*Graduate School of Advanced Science and Engineering, Hiroshima University, 1-3-1 Kagamiyama, Higashi-Hiroshima, Hiroshima 739-8526, Japan*

[c]*Office of Research and Academia-Government-Community Collaboration, Hiroshima University, 1-3-2 Kagamiyama, Higashi-Hiroshima, Hiroshima 739-8511, Japan*

[d]*Biotechnology Research Center, Toyama Prefectural University, 5180 Kurokawa, Imizu, Toyama 939-0398, Japan*

[e]*Graduate School of Science, Osaka University, 1-1 Machikaneyama-cho, Toyonaka, Osaka 560-0043, Japan*

[f]*RIKEN Cluster for Pioneering Research, 2-1 Hirosawa, Wako, Saitama 351-0198, Japan*

[g]*Institute for Glyco-core Research (iGCORE), Nagoya University, Furo-cho, Chikusa-ku, Nagoya 464-8601, Japan*

*Corresponding author
E-mail address: yu@agr.nagoya-u.ac.jp (Y. Nakagawa)

ABSTRACT

Pradimicin A (PRM-A) and its derivatives comprise a unique family of antibiotics that show antifungal, antiviral, and antiparasitic activities through binding to D-mannose (Man)-containing glycans of pathogenic species. Despite their great potential as drug leads with an exceptional antipathogenic action, therapeutic application of PRMs has been severely limited by their tendency to form water-insoluble aggregates. Recently, we found that attachment of 2-aminoethanol to the carboxy group of PRM-A *via* amide linkage significantly suppressed the aggregation. Here, we prepared additional amide derivatives (**2**–**8**) of PRM-A to examine the possibility that the amide formation of PRM-A could suppress its aggregation propensity. Sedimentation assay and isothermal titration calorimetry experiment confirmed that all amide derivatives can bind Man without significant aggregation. Among them, hydroxamic acid derivative (**4**) showed the most potent Man-binding activity, which was suggested to be derived from the anion formation of the hydroxamic acid moiety by molecular modeling. Derivative **4** also exhibited significant antifungal activity comparable to that of PRM-A. These results collectively indicate that amide formation of PRM-A is the promising strategy to develop less aggregative derivatives, and **4** could serve as a lead compound for exploring the therapeutic application of PRM-A.

1. Introduction

Pradimicins (PRMs, Fig. 1) are a structurally and biologically unique family of antibiotics derived from actinomycetes.[1–3] PRMs exhibit potent antimicrobial activity both *in vitro* and *in vivo* against a wide range of fungi and yeasts, including clinically harmful *Candida albicans*, *Aspergillus fumigatus*, *Cryptococcus neoformans*, and *Fusarium moniliforme*.[4,5] Significantly, they have little toxicity against various mammalian cells, and there is no cross-resistance to the major antimicrobial agents, such as amphotericin B, 5-fluorocytosine, and ketoconazole. These therapeutically promising observations have justifiably driven interest in their mode of action, and intensive studies have revealed that the antifungal action of PRMs originates from their Ca^{2+}-dependent binding to D-mannose (Man) residues of cell wall mannans.[6,7]

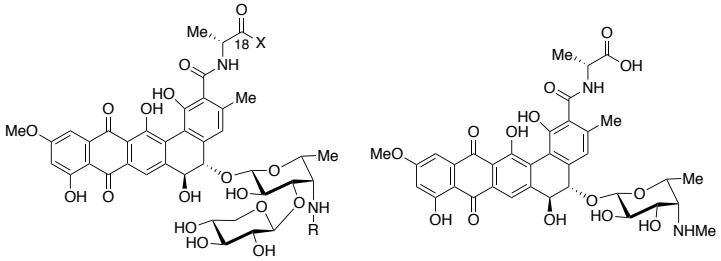

Fig. 1. Structures of pradimicins and amide derivative **1**.

The finding on the lectin-like ability of PRMs has further led to the demonstration that they also show antiviral and antiparasitic activities against human immunodeficiency virus (HIV), dengue virus, hepatitis C virus, coronavirus, and protozoan parasite *Trypanosoma brucei* by binding to Man-containing glycans of these pathogenic species.[8–13] Such glycan-targeted antipathogenic behavior is not observed in major classes of existing chemotherapeutics, highlighting their potential as drug leads with a novel mode of action. However, therapeutic application of PRMs has yet to be realized. One of the major obstacles is their tendency to form

aggregates in the presence of Ca^{2+}. Early studies found that the actual Man-binding species is the [PRM_2/Ca^{2+}] complex (Scheme 1), which is highly cohesive to form water-insoluble aggregates.[14–16] The aggregation of the [PRM_2/Ca^{2+}] complex is reported to occur at 1 mM $CaCl_2$ in neutral aqueous solutions,[14] which corresponds to serum ionized Ca^{2+} concentration (1.1–1.2 mM).[17] This unfavorable property has hampered further studies on medicinal use of PRMs.

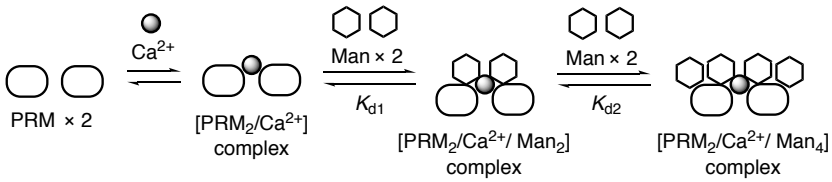

Scheme 1. Complex formation of PRMs with Ca^{2+} and Man. Two PRM molecules are initially bridged by Ca^{2+} to form the [PRM_2/Ca^{2+}] complex, which binds two molecules of Man with high affinity. The resulting [$PRM_2/Ca^{2+}/Man_2$] complex accommodates another two molecules of Man with low affinity to afford the [$PRM_2/Ca^{2+}/Man_4$] complex. The [PRM_2/Ca^{2+}] complex along with the [$PRM_2/Ca^{2+}/Man_2$] and [$PRM_2/Ca^{2+}/Man_4$] complexes have a high aggregation propensity to form water-insoluble aggregates. K_{d1} and K_{d2} represent the dissociation constants for primary and secondary Man binding, respectively.

Recently, our solid-state NMR-based density functional theory (DFT) calculations provided a reliable estimation of the [$PRM_2/Ca^{2+}/Man_2$] complex, which led to the finding that amide formation at the C18 carboxy group of PRMs did not have a major deleterious effect on Man binding.[18] Of greater significance is the demonstration that the 2-hydroxyethylamide derivative (**1**, Fig. 1) of PRM-A hardly showed any aggregation in Ca^{2+}-containing aqueous solutions,[19] raising the possibility that amide formation at the C18 carboxy group of PRM-A could be a promising modification strategy to suppress the aggregation. In this study, we validate this possibility by evaluating additional amide derivatives of PRM-A for their aggregation properties and Man binding affinities. We also examined their antifungal activity against *Candida rugosa* to evaluate their potential as lead compounds for the development of antifungal drugs.

2. Results and discussion

*2.1. Aggregation property of amide derivatives **2**–**8***

We initially prepared simple amide derivatives (**2**, **3**)[20] to examine the contribution of the hydroxyethyl moiety of **1** on mitigation of the aggregate-forming propensity (Scheme 2). These derivatives were readily synthesized from PRM-A through methyl esterification followed by ester/amide exchange reaction. The aggregate-forming properties of **2** and **3** were evaluated *via* a sedimentation assay.[19] After incubation of 0.2, 0.5, or 1.0 mM PRMs in 50 mM 3-morpholinopropane-1-sulfonic acid (MOPS) buffer (pH 7.0) containing 10 mM $CaCl_2$ at 37 °C for 15 min followed by centrifugation, the residual amounts of PRMs in the supernatant were measured by HPLC analysis. As shown in Fig. 2, while PRM-A was hardly detected in the supernatant due to severe aggregation, **2** and **3** were markedly less aggregative and more than 60% of them remained in the supernatant even at 1.0 mM. Although the residual amounts of **2** and **3** in the supernatant were slightly lower than that of **1**, these results suggest that the hydroxyethyl moiety of **1** has a marginal role and the amide formation mainly contributes to the mitigation of the aggregate-forming propensity.

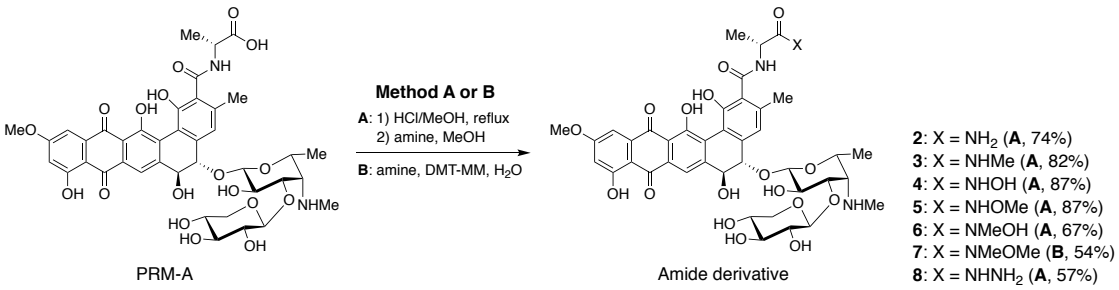

Scheme 2. Synthesis of amide derivatives (**2**–**8**). The amide derivatives were prepared from PRM-A by ester/amide exchange reaction (method A) or condensation reaction (method B).

This finding prompted us to prepare additional derivatives (**4**–**8**) with hydroxyamide or hydrazide functionalities (Scheme 2). All derivatives except for **7** were obtained by ester/amide

exchange reaction using PRM-A methyl ester and corresponding amines. In the synthesis of **7**, PRM-A methyl ester was unreactive to *N*,*O*-dimethylhydroxylamine, and thus **7** was obtained by dehydrating condensation of PRM-A with *N*,*O*-dimethylhydroxylamine by using 4-(4,6-dimethoxy-1,3,5-triazin-2-yl)-4-methylmorpholinium chloride (DMT-MM)[21] as a coupling reagent. Derivatives **4**–**8** were then evaluated for their aggregation property. As shown in Fig. 2, 65–85% of **4**–**8** remained in the supernatant, and precipitation was not observed at any concentration. These results strongly support that the amide formation at the C18 carboxy group is a promising strategy for suppressing the aggregation of PRM-A. Although the origin of less aggregation of the amide derivatives remains to be elucidated, one possible explanation is that the salt bridge formation between the C18 carboxy and the C4' amino groups of PRMs contributes to aggregate formation, which would be inhibited by amide formation at the C18 carboxy group (Fig. 3).

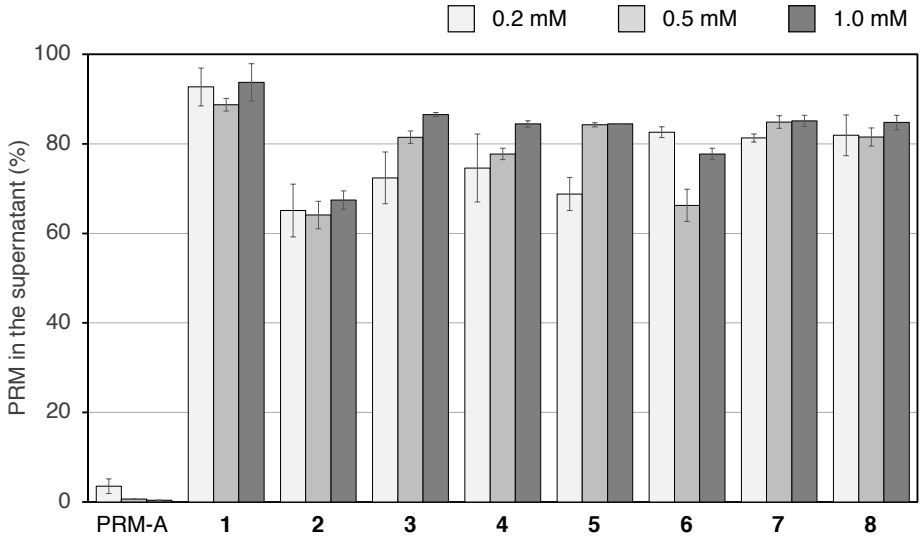

Fig. 2. Aggregation of PRM-A and amide derivatives **1**–**8** in Ca^{2+}-containing neutral aqueous media. The sedimentation assay was carried out using 0.2, 0.5, or 1.0 mM PRMs in 50 mM MOPS buffer (pH 7.0) containing 10 mM $CaCl_2$. The amounts of PRMs in the supernatant were estimated from HPLC peak areas and expressed as a percentage of the control.

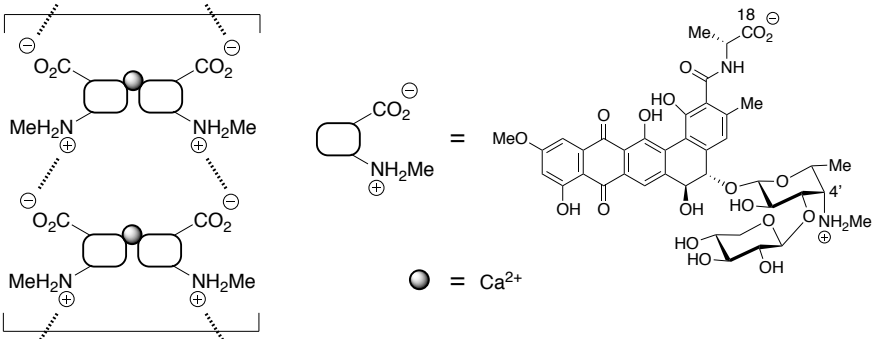

Fig. 3. Putative mechanism of salt bridge-mediated aggregation of PRMs. PRM molecules are accumulated through salt bridge between their C18 carboxy and the C4' amino groups. Amide formation at the C18 carboxy group inhibits the salt bridge formation, resulting in suppression of the aggregate formation.

*2.2. Man-binding affinity of amide derivatives **2**–**8***

Following the confirmation that amide derivatives **2**–**8** are not cohesive, we subsequently evaluated their Man-binding ability by isothermal titration calorimetry (ITC) experiments using methyl α-D-mannopyranoside (Man-OMe). Table 1 summarizes the dissociation constants of **2**–**8** for the primary (K_{d1}) and secondary (K_{d2}) Man-OMe binding (Scheme 1). The results of PRM-A[22] and **1**[19] are also listed for comparison. While binding affinity of *N*-methylamide derivative (**3**) for Man-OMe was slightly weak, the other derivatives (**2**, **4**–**8**) exhibited higher affinity than that of 2-hydroxyethylamide derivative (**1**), indicating a negative effect of the hydroxyethyl moiety of **1** on Man binding. It is also noteworthy that Man-binding potency of hydroxamic acid derivative (**4**) was comparable or even higher than that of PRM-A. Additional ITC experiments demonstrated that like PRM-A, **4** can discriminate Man from other common monosaccharides including D-glucose, D-galactose, *N*-acetyl-D-glucosamine, and *N*-acetylneuraminic acid. These results collectively confirm that amide formation at the C18 carboxy group of PRM-A does not have a major deleterious effect on binding affinity and selectivity for Man, and also suggest that the hydroxamic acid moiety of **4** would make a positive contribution to its interaction with Man.

Table 1. Dissociation constants of PRMs for the primary (K_{d1}) and secondary (K_{d2}) Man-OMe binding

PRM	K_{d1} (μM) ± error of fit[a]	K_{d2} (μM) ± error of fit[a]
PRM-A	96[b]	3,800[b]
1	650[c]	6,300[c]
2	220 ± 14	5,500 ± 230
3	860 ± 140	6,500 ± 510
4	75 ± 3.1	4,300 ± 170
5	360 ± 40	5,300 ± 370
6	180 ± 34	3,500 ± 370
7	340 ± 39	5,200 ± 360
8	300 ± 28	9,800 ± 630

[a]Determined by ITC experiments. [b]Data cited from ref. 22. [c]Data cited from ref. 19.

Table 2. Dissociation constants of **4** for the primary (K_{d1}) and secondary (K_{d2}) monosaccharide binding

Monosaccharide	K_{d1} (μM) ± error of fit[a]	K_{d2} (μM) ± error of fit[a]
D-Mannose	100 ± 7.9	5,500 ± 340
D-Glucose	–[b]	–[b]
D-Galactose	–[b]	–[b]
N-Acetyl-D-glucosamine	–[b]	–[b]
N-Acetylneuraminic acid[c]	–[b]	–[b]

[a]Determined by ITC experiments. [b]Too large to be determined. [c]*N*-Acetylneuraminic acid methyl ester was used to avoid severe pH changes during titration.

*2.3. Possible mode of Man binding of **4***

To estimate the contribution of the hydroxamic acid moiety to Man binding of **4**, we performed molecular modeling. Given that hydroxamic acids easily form hydroxamates by deprotonation, initial structures were proposed for the [$\mathbf{4}_2$/Ca^{2+}/(Man-OMe)$_2$], [$\mathbf{4a}_2$/Ca^{2+}/(Man-OMe)$_2$], and [$\mathbf{4b}_2$/Ca^{2+}/(Man-OMe)$_2$] complexes based on the previously estimated structure of the [PRM-A_2/Ca^{2+}/(Man-OMe)$_2$] complex,[18] followed by optimization through DFT calculations at the ωB97X-D/6-31G(d) level of theory (Fig. 4). The interaction energy (E_{int}) of [$\mathbf{4}_2$/Ca^{2+}], [$\mathbf{4a}_2$/Ca^{2+}], and [$\mathbf{4b}_2$/Ca^{2+}] complexes with two molecules of Man-OMe is also shown in Fig. 4B.

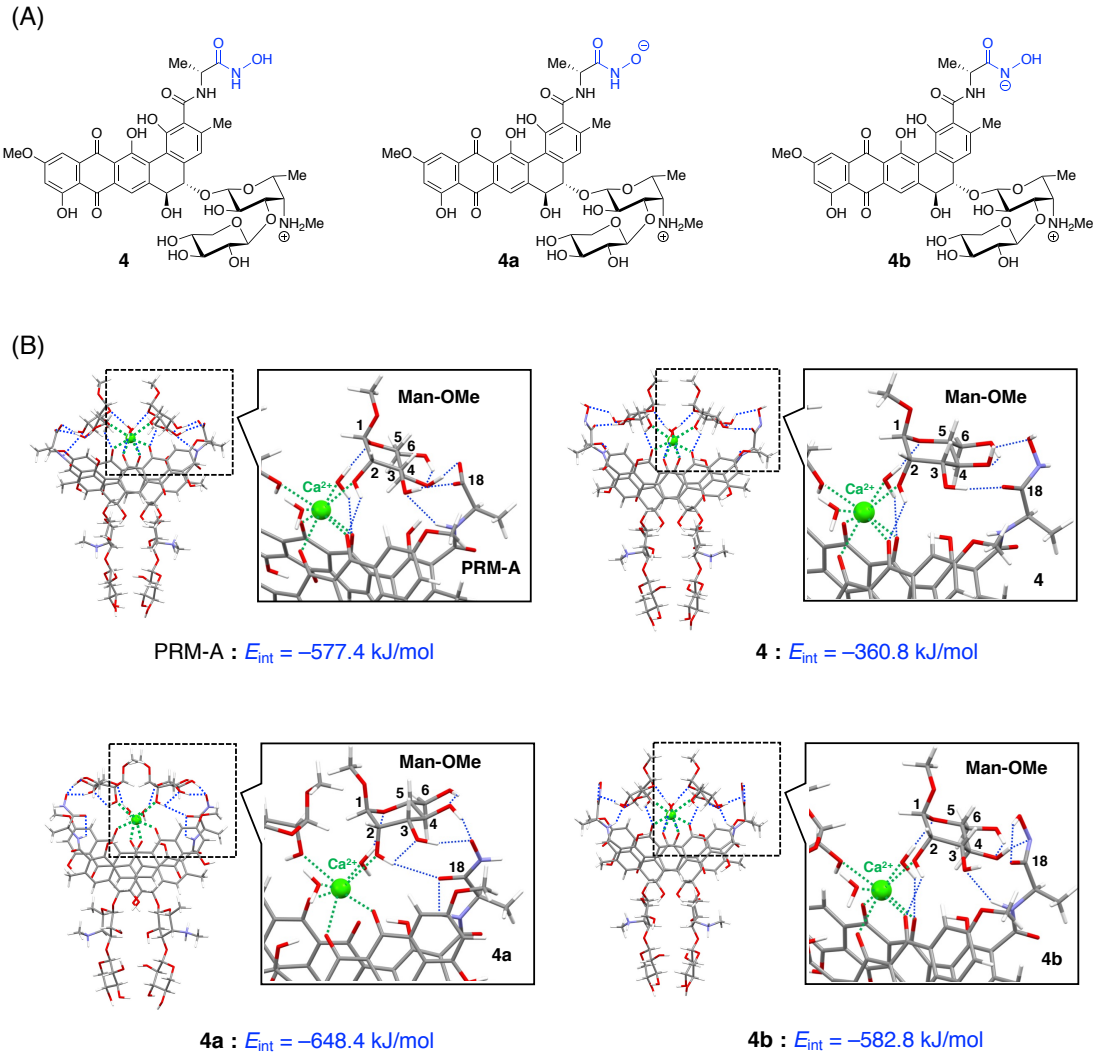

Fig. 4. Possible mode of Man binding of **4**. (A) Structures of **4** and its hydroxamate forms (**4a**, **4b**) used for molecular modeling. (B) Energy-minimized structures of the [PRM-A$_2$/Ca^{2+}/(Man-OMe)$_2$],[18] [**4**$_2$/Ca^{2+}/(Man-OMe)$_2$], [**4a**$_2$/Ca^{2+}/(Man-OMe)$_2$], and [**4b**$_2$/Ca^{2+}/(Man-OMe)$_2$] complexes by DFT calculations. Carbon, oxygen, nitrogen, hydrogen, and calcium atoms are shown in gray, red, blue, and green, respectively. Hydrogen bonding and Ca^{2+} coordination are indicated as blue and green dotted lines, respectively. E_{int} represents interaction energy of [PRM-A$_2$/Ca^{2+}], [**4**$_2$/Ca^{2+}], [**4a**$_2$/Ca^{2+}], or [**4b**$_2$/Ca^{2+}] complexes with two molecules of Man-OMe.

The complex structures show that, as in the case of PRM-A, **4** and its hydroxamate forms (**4a**, **4b**) all interact with the 2-, 3-, and 4-hydroxy groups of Man-OMe but not with its 6-hydroxy

group and 1-methoxy groups. However, the E_{int} values are significantly different between protonated (**4**) and deprotonated (**4a**, **4b**) forms. More specifically, the absolute value of E_{int} decreases in the following order: **4a** > **4b** ≥ PRM-A >> **4**, suggesting that **4a** and **4b** would bind Man-OMe more strongly than **4** and PRM-A. When considering the slightly higher affinity of **4** (K_{d1} = 75 μM) for Man-OMe compared to that of PRM-A (K_{d1} = 96 μM), it is quite likely that **4** binds Man-OMe as a hydroxamate form (**4a** or **4b**). This assumption is supported by the attenuated binding affinity of *N*,*O*-dimethyl hydroxamic acid derivative **7** (K_{d1} = 340 μM), which has no dissociable proton at the hydroxamic acid moiety. When comparing mono-methylated derivatives (**5**, **6**), *O*-methylated **5** (K_{d1} = 360 μM) showed weaker affinity than *N*-methylated **6** (K_{d1} = 180 μM), suggesting a major contribution of **4a** to Man binding. A slight decrease in binding affinity by *N*-methylation of **4** (K_{d1} = 75 μM for **4**, K_{d1} = 180 μM for **6**) could be possibly explained by the lower acidity of *N*-methylated hydroxamic acids compared with non-methylated ones,[23,24] further supporting that dissociation of the OH group at the hydroxamic acid moiety of **4** has a positive impact on Man binding affinity.

*2.4. Antifungal activity of amide derivatives **2**–**8***

Following the confirmation that amide derivatives bind Man without severe aggregation, we then evaluated their antifungal activity against *Candida rugosa*. As shown in Table 3, all derivatives prevented fungal growth. Among them, **4** was found to be the most potent antifungal agent with a MIC (minimum inhibitory concentration) value of 8 μg/mL, approaching that of PRM-A (MIC = 4 μg/mL). Given that binding of PRMs to cell wall mannans of fungi is the initial step triggering their antifungal action,[1,6] the potency of **4** might be partly derived from its higher affinity for Man (K_{d1} = 75 μM) compared to other amide derivatives (K_{d1} = 180–860 μM).

Table 3. MIC values of PRMs against *Candida rugosa*

PRM	MIC[a] (μg/mL)
PRM-A	4
1	16
2	16
3	16
4	8
5	16
6	16
7	16
8	16

[a]Minimum inhibitory concentration.

3. Conclusions

In this study, seven amide derivatives of PRM-A (**2**–**8**) were prepared and evaluated for their aggregative property, Man binding affinity, and antifungal activity. The results collectively support our assumption that amide formation at the C18 carboxy group of PRM-A can effectively suppress the aggregative propensity without abolishing Man binding and antifungal activities. Of the amide derivatives tested, **4** was comparable to PRM-A at binding Man-OMe and preventing fungal growth. Given these biological activities and less aggregative propensity, **4** is better suitable for therapeutic application than PRM-A. The issue that remains to be examined is why antifungal activity of **4** was not so strong despite its higher affinity for Man relative to PRM-A. We previously demonstrated that binding of PRMs to fungal mannans originates from the recognition of oligomannose units rather than from that of single Man units,[25] raising the possibility that oligomannose binding of **4** might be weaker than that of PRM-A. Further investigation on this issue and therapeutic optimization of **4** is current underway and will be reported in due course.

4. Experimental

4.1. General remarks

PRM-A was isolated from the fermentation broth of *Actinomadura* sp. TP-A0019 as reported previously.[26] PRM-A methyl ester was prepared according to the reported method.[20] HPLC was carried out using an L-2130 HPLC system (Hitachi). NMR spectra were measured on a Bruker AVANCE 400 (^{1}H at 400 MHz, ^{13}C at 100 MHz) magnetic resonance spectrometer. ^{1}H chemical shifts are reported relative to the residual solvent peak (DMSO = 2.50 ppm). ^{13}C chemical shifts are reported relative to the residual deuterated solvent ^{13}C signals (DMSO = 39.52 ppm). Signal assignments were made *via* 2D spectroscopy (COSY, HSQC, and HMBC). Optical rotation data were obtained using a JASCO DIP-370 digital polarimeter. High-resolution mass spectrum was obtained using an Applied Biosystems Mariner ESI-TOF spectrometer. Chemical reagents were purchased from commercial suppliers (Kanto Chemical, Sigma-Aldrich, TCI Chemicals, Wako Pure Chemical Industries) and were used as received without additional purification.

4.2. Derivative synthesis

*Synthesis and Characterization of **2***

To a solution of PRM-A (TFA salt, 235 mg, 0.25 mmol) in MeOH (40 mL) was added 10% HCl methanol solution (0.85 mL). The reaction mixture was refluxed at 80 ºC for 2.5 hours, and then directly loaded onto Waters Sep-Pak® (Vac 35cc C_{18}-5g). After washing with H_2O containing 0.1% TFA, the gel was eluted with 50% MeCN/H_2O containing 0.1% TFA and the eluate was concentrated *in vacuo* to afford crude PRM-A Me ester (244 mg, 0.25 mmol, quant.) as a TFA salt. The crude PRM-A methyl ester (TFA salt, 19.4 mg, 20.0 μmol) was dissolved in MeOH (2.0 mL), and 28% ammonia solution (0.068 mL, 10.0 mmol, 500 equiv.) was added. The reaction

mixture was stirred at room temperature for 16 hours, and then directly loaded onto Waters Sep-Pak® (Vac 35cc C_{18}-5g). After washing with H_2O containing 0.1% TFA, the gel was eluted with 50% MeCN/H_2O containing 0.1% TFA and the eluate was concentrated *in vacuo*. The residue was purified by reverse phase HPLC (system: Hitachi L-2130, column: YMC-Pack ODS-A, 5 μm, 20.0 mm ID x 250 mm; solvent: 40 min linear gradient 25–50% CH_3CN/H_2O containing 0.1% TFA; flow rate: 8.0 mL/min; UV: 254 nm; Rt: 25.8 min) to afford **2** (14.2 mg, 14.9 μmol, 74%; two-step yield from PRM-A) as a TFA salt.

$[\alpha]_D$: –864 (*c* = 0.102 in MeOH, 26˚C); ^{1}H-NMR (400 MHz, DMSO-d_6): δ = 1.30 (d, 6.8 Hz, 3H), 1.34 (d, 7.2 Hz, 3H), 2.30 (s, 3H), 2.70 (s, 3H), 3.12-3.21 (m, 3H), 3.31-3.37 (m, 1H), 3.45 (d, 2.8 Hz, 1H), 3.53 (s, br, 1H), 3.77 (dd, 5.2, 11.2 Hz, 1H), 3.93 (q, 6.8 Hz, 1H), 3.97 (s, 3H), 3.99 (dd, 2.8, 6.4 Hz, 1H), 4.43 (q, 7.2 Hz, 1H), 4.49 (d, 7.2 Hz, 1H), 4.62 (d, 8.4 Hz, 1H), 4.69 (d, 8.4 Hz, 1H), 4.78 (d, 7.6 Hz, 1H), 6.92 (d, 2.0 Hz 1H), 7.13 (s, 1H), 7.32 (d, 2.0 Hz, 1H), 8.02 (s, 1H), 8.21 (d, 7.2 Hz, 1H, NH); ^{13}C-NMR (100 MHz, DMSO-d_6): δ = 15.8, 17.4, 18.8, 36.0, 48.2, 56.2, 63.0, 65.7, 67.2, 69.2, 69.6, 71.0, 73.3, 75.7, 79.3, 80.6, 103.7, 104.9, 106.6, 107.4, 110.0, 114.4, 115.8, 116.3, 119.4, 126.4, 127.6, 131.3, 134.5, 136.6, 137.3, 147.2, 151.4, 157.5, 164.6, 165.9, 166.7, 174.2, 185.0, 186.8; HRMS (ESI) : *m/z* = 862.2644 ($[M+Na]^+$). Calcd. For $C_{40}H_{45}N_3NaO_{17}^+$ 862.2641.

*Synthesis and Characterization of **3***

To a solution of the crude PRM-A methyl ester (TFA salt, 21.6 mg, 22.3 μmol) in MeOH (2.2 mL) was added 40% methylamine in MeOH (1.14 mL, 11.2 mmol, 500 equiv.). The reaction mixture was stirred at room temperature for 15 hours, and then directly loaded onto Waters Sep-Pak® (Vac 35cc C_{18}-2g). After washing with H_2O containing 0.1% TFA, the gel was eluted with 50% MeCN/H_2O containing 0.1% TFA and the eluate was concentrated *in vacuo*. The residue was

purified by reverse phase HPLC (system: Hitachi L-2130, column: YMC-Pack ODS-A, 5 μm, 20.0 mm ID x 250 mm; solvent: 40 min linear gradient 25–50% CH_3CN/H_2O containing 0.1% TFA; flow rate: 8.0 mL/min; UV: 254 nm; Rt: 27 min) to afford **3** (17.6 mg, 18.2 μmol, 82%; two-step yield from PRM-A) as a TFA salt.

$[\alpha]_D$: +661 (*c* = 0.109 in MeOH, 26˚C); ^{1}H-NMR (400 MHz, DMSO-d_6): δ = 1.29 (d, 6.8 Hz, 3H), 1.33 (d, 7.4 Hz, 3H), 2.30 (s, 3H), 2.65 (s, 3H), 2.69 (s, 3H), 3.11-3.21 (m, 3H), 3.33 (m, 1H), 3.44 (d, 4.2 Hz, 1H), 3.56 (s, br, 1H), 3.77 (dd, 5.2, 11.2 Hz, 1H), 3.92 (q, 6.8 Hz, 1H), 3.95 (s, 3H), 3.98 (dd, 4.2, 6.0 Hz, 1H), 4.45 (q, 7.4 Hz, 1H), 4.50 (d, 8.8 Hz, 1H), 4.61 (d, 8.8 Hz, 1H), 4.68 (d, 8.8 Hz, 1H), 4.76 (d, 7.6 Hz, 1H), 6.91 (d, 2.4 Hz 1H), 7.16 (s, 1H), 7.31 (d, 2.4 Hz, 1H), 8.04 (s, 1H), 8.22 (d, 7.4 Hz, 1H, NH); ^{13}C-NMR (100 MHz, DMSO-d_6): δ = 16.0, 17.6, 19.0, 25.5, 36.0, 48.5, 56.4, 63.1, 65.7, 67.4, 67.9, 69.2, 69.7, 71.1, 73.3, 75.7, 79.1, 80.7, 103.8, 104.8, 106.9, 107.7, 110.1, 114.16, 114.20, 115.8, 115.9, 125.9, 127.6, 131.5, 134.5 137.0, 137.6, 147.7, 150.9, 156.7, 164.4, 166.1, 166.9, 172.6, 185.0, 187.4; HRMS (ESI) : *m/z* = 876.2796 ($[M+Na]^+$). Calcd. For $C_{41}H_{47}N_3NaO_{17}^+$ 876.2796.

*Synthesis and Characterization of **4***

A suspension of hydroxylamine hydrochloride (3.2 g, 0.046 mmol) in MeOH (16.3 mL) was refluxed under N_2 until a clear solution was obtained. A solution of KOH (4.6 g, 0.082 mmol) in MeOH (9.5 mL) was then added, and the whole mixture was refluxed for 30 min. After cooling to room temperature, the resulting NH_2OK solution (0.63 mL, 1.11 mmol, 50 equiv.) was added to a solution of the crude PRM-A methyl ester (TFA salt, 21.6 mg, 22.3 μmol) in MeOH (12.0 mL). The reaction mixture was stirred at room temperature for 2 hours, and then directly loaded onto Waters Sep-Pak® (Vac 35cc C_{18}-2g). After washing with H_2O containing 0.1% TFA, the gel was eluted with 50% $MeCN/H_2O$ containing 0.1% TFA and the eluate was concentrated *in vacuo*.

The residue was purified by reverse phase HPLC (system: Hitachi L-2130, column: YMC-Pack ODS-A, 5 μm, 20.0 mm ID x 250 mm; solvent: 40 min linear gradient 25–50% CH_3CN/H_2O containing 0.1% TFA; flow rate: 8.0 mL/min; UV: 254 nm; Rt: 22.0 min) to afford **4** (18.8 mg, 19.4 μmol, 87%; two-step yield from PRM-A) as a TFA salt.

$[\alpha]_D$: +107 (c = 0.273 in MeOH, 27 °C); ^{1}H-NMR (600 MHz, DMSO-d_6): δ = 1.31 (d, 6.4 Hz, 3H), 1.33 (d, 7.2 Hz, 3H), 2.31 (s, 3H), 2.71 (s, 3H), 3.13-3.23 (m, 3H), 3.35 (m, 1H), 3.46 (m, 1H), 3.57 (m, br, 1H), 3.78 (dd, 5.2, 11.2 Hz, 1H), 3.93 (q, 6.4 Hz, 1H), 3.98 (s, 3H), 4.00 (dd, 4.0, 6.0 Hz, 1H), 4.45 (m, 1H), 4.51 (d, 6.8 Hz, 1H), 4.62 (d, 8.8 Hz, 1H), 4.68 (d, 8.8 Hz, 1H), 4.79 (d, 7.6 Hz, 1H), 6.92 (d, 2.0 Hz, 1H), 7.13 (s, 1H), 7.32 (d, 2.0 Hz, 1H), 8.04 (s, 1H), 8.18 (d, 4.4 Hz, 1H); ^{13}C-NMR (150 MHz, DMSO-d_6): δ = 16.0, 17.9, 19.1, 36.1, 48.4, 56.4, 63.0, 65.7, 67.3, 69.2, 69.8, 71.4, 73.4, 75.7, 79.1, 80.7, 103.8, 104.8, 106.7, 107.6, 110.1, 114.0, 114.5, 115.7, 117.9, 125.9, 127.4, 131.4, 134.5, 137.0, 137.6, 147.6, 151.1, 157.0, 164.7, 166.7, 167.5, 169.1, 185.0, 187.3; HRMS (ESI) : m/z = 878.2597 ($[M+Na]^+$). Calcd. For $C_{40}H_{45}N_3NaO_{18}^+$ 878.2590.

*Synthesis and Characterization of **5***

A suspension of *O*-methylhydroxylamine hydrochloride (3.8 g, 0.045 mmol) in MeOH (16.2 mL) was refluxed under N_2 until a clear solution was obtained. A solution of KOH (2.9 g, 0.052 mmol) in MeOH (9.5 mL) was then added, and the whole mixture was refluxed for 30 min. After cooling to room temperature, the resulting NH_2OMe solution (12.6 mL, 22.1 mmol, 500 equiv.) was added to a solution of the crude PRM-A methyl ester (TFA salt, 42.8 mg, 44.2 μmol) in MeOH (8.0 mL). The reaction mixture was stirred at room temperature for 8 hours, and then directly loaded onto Waters Sep-Pak® (Vac 35cc C_{18}-2g). After washing with H_2O containing 0.1% TFA, the gel was eluted with 50% $MeCN/H_2O$ containing 0.1% TFA and the eluate was concentrated *in vacuo*. The

residue was purified by reverse phase HPLC (system: Hitachi L-2130, column: YMC-Pack ODS-A, 5 μm, 20.0 mm ID x 250 mm; solvent: 40 min linear gradient 25–50% CH_3CN/H_2O containing 0.1% TFA; flow rate: 8.0 mL/min; UV: 254 nm; Rt: 23.1 min) to afford **5** (37.8 mg, 38.4 μmol, 87%; two-step yield from PRM-A) as a TFA salt.

$[\alpha]_D$: –1.0 (*c* = 0.261 in MeOH, 26 ºC); ^{1}H-NMR (600 MHz, DMSO-d_6): δ = 1.28 (d, 6.6 Hz, 3H), 1.30 (d, 7.2 Hz, 3H), 2.28 (s, 3H), 2.69 (s, 3H), 3.12-3.20 (m, 3H), 3.31-3.34 (m, 1H), 3.45 (d, 3.9 Hz, 1H), 3.53 (s, br, 1H), 3.63 (s, 3H), 3.77 (dd, 5.4, 11.4 Hz, 1H), 3.91 (q, 6.6 Hz, 1H), 3.95 (s, 3H), 4.00 (dd, 3.9, 7.2 Hz, 1H), 4.36 (m, 1H), 4.46 (d, 7.2 Hz, 1H), 4.60 (d, 8.7 Hz, 1H), 4.65 (d, 8.7 Hz, 1H), 4.77 (d, 7.2 Hz, 1H), 6.90 (d, 2.1 Hz 1H), 7.13 (s, 1H), 7.30 (d, 2.1 Hz, 1H), 8.03 (s, 1H), 8.29 (d, 6,6 Hz, 1H, NH); ^{13}C-NMR (150 MHz, DMSO-d_6): δ = 16.5, 18.0, 19.6, 36.6, 47.0, 56.9, 63.6, 63.7, 66.3, 67.9, 69.7, 70.2, 71.8, 73.9, 76.3, 80.0, 81.2, 104.3, 105.5, 107.3, 108.1, 110.6 114.6, 114.8, 116.4, 116.6, 126.6, 128.0, 132.0, 135.1, 137.6, 138.1, 148.0, 151.8, 157.6, 164.9, 166.6, 167.5, 169.6, 185.6, 187.7; HRMS (ESI) : *m/z* = 870.2918 ($[M+H]^+$). Calcd. For $C_{41}H_{48}N_3O_{18}^+$ 870.2927.

Synthesis and Characterization of ***6***

A suspension of *N*-methylhydroxylamine hydrochloride (3.0 g, 0.036 mmol) in MeOH (13.0 mL) was refluxed under N_2 until a clear solution was obtained. A solution of KOH (2.3 g, 0.041 mmol) in MeOH (7.6 mL) was then added, and the whole mixture was refluxed for 30 min. After cooling to room temperature, and the resulting NH(Me)OH solution (24.1 mL, 42.1 mmol, 1300 equiv.) was directly added to the crude PRM-A methyl ester (TFA salt, 31.4 mg, 32.4 μmol). The reaction mixture was stirred at room temperature for 22 hours, and then directly loaded onto Waters Sep-Pak® (Vac 35cc C_{18}-2g). After washing with H_2O containing 0.1% TFA, the gel was eluted with 50% $MeCN/H_2O$ containing 0.1% TFA and the eluate was concentrated *in vacuo*. The residue was

purified by reverse phase HPLC (system: Hitachi L-2130, column: YMC-Pack ODS-A, 5 μm, 20.0 mm ID x 250 mm; solvent: 40 min linear gradient 25–50% CH_3CN/H_2O containing 0.1% TFA; flow rate: 8.0 mL/min; UV: 254 nm; Rt: 26.3 min) to afford **6** (21.4 mg, 21.8 μmol, 67%; two-step yield from PRM-A) as a TFA salt.

$[\alpha]_D$: +46 (*c* = 0.313 in MeOH, 29 ºC); ^{1}H-NMR (600 MHz, DMSO-d_6): δ = 1.29 (d, 6.6 Hz, 3H), 1.33 (d, 6.9 Hz, 3H), 2.31 (s, 3H), 2.69 (s, 3H), 3.12-3.20 (m, 3H), 3.16 (s, 3H), 3.31 (m, 1H), 3.45 (d, 3.7 Hz, 1H), 3.54 (s, br, 1H), 3.77 (dd, 5.4, 11.4 Hz, 1H), 3.92 (q, 1H), 3.95 (s, 3H), 3.98 (dd, 3.7, 8.4 Hz, 1H), 4.48 (d, 7.2 Hz, 1H), 4.60 (d, 8.4 Hz, 1H), 4.65 (d, 8.4 Hz, 1H), 4.78 (d, 7.2 Hz, 1H), 5.04 (q, 6.9 Hz, 1H), 6.90 (d, 1.8 Hz 1H), 7.12 (s, 1H), 7.30 (d, 1.8 Hz, 1H), 8.02 (s, 1H); ^{13}C-NMR (150 MHz, DMSO-d_6): δ = 16.5, 17.4, 19.8, 36.6, 36.7, 45.8, 56.9, 63.6, 66.3, 67.9, 69.7, 70.2, 71.9, 73.9, 76.3, 80.0, 81.2, 104.3, 105.5, 107.2, 108.1, 110.7, 114.7, 114.8, 116.3, 116.8, 126.7, 127.6, 132.0, 135.2, 137.7, 138.1, 148.0, 151.9, 157.8, 164.9, 166.6, 167.2, 172.8, 185.6, 187.7; HRMS (ESI) : *m/z* = 870.2923 ($[M+H]^+$). Calcd. For $C_{41}H_{48}N_3O_{18}^+$ 870.2927.

Synthesis and Characterization of 7

To a solution of PRM-A (TFA salt, 43.4 mg, 45.5 μmol) in H_2O (6.5 mL) were added *N*,*O*-dimethylhydroxylamine hydrochloride (221 mg, 2.27 mmol, 50 equiv.), KOH (134 mg, 2.39 mmol, 52.5 mmol) and DMT-MM (157 mg, 0.57 mmol, 12.5 equiv.). The reaction mixture was stirred at room temperature for 19 hours, and then directly loaded onto Waters Sep-Pak® (Vac 35cc C_{18}-2g). After washing with H_2O containing 0.1% TFA, the gel was eluted with 50% MeCN/H_2O containing 0.1% TFA and the eluate was concentrated *in vacuo*. The residue was purified by reverse phase HPLC (system: Hitachi L-2130, column: YMC-Pack ODS-A, 5 μm, 20.0 mm ID x 250 mm; solvent: 40 min linear gradient 25–50% CH_3CN/H_2O containing 0.1% TFA; flow rate: 8.0 mL/min; UV: 254 nm; Rt: 34.3 min) to afford **7** (21.6 mg, 24.4 μmol, 54%)

as a TFA salt.

$[\alpha]_D$: +146 (*c* = 0.244 in MeOH, 28 °C); ^{1}H-NMR (600 MHz, DMSO-d_6): δ = 1.31 (d, 7.2 Hz, 3H,), 1.31 (d, 7.2 Hz, 3H), 2.33 (s, 3H), 2.71 (s, 3H), 3.13-3.21 (m, 3H), 3.18 (s, 3H), 3.31-3.34 (m, 1H), 3.47 (d, 3.9 Hz, 1H), 3.57 (s, br, 1H), 3.78 (dd, 5.4, 11.4 Hz, 1H), 3.82 (s, 3H), 3.93 (q, 7.2 Hz, 1H,), 3.97 (s, 3H), 4.00 (dd, 3.9, 7.8 Hz, 1H), 4.50 (d, 7.2 Hz, 1H), 4.62 (d, 8.7 Hz, 1H), 4.65 (d, 8.7 Hz, 1H), 4.80 (d, 7.2 Hz, 1H), 4.94 (q, 7.2 Hz, 1H), 6.93 (d, 1.2 Hz 1H), 7.14 (s, 1H), 7.33 (d, 2.1 Hz, 1H), 8.05 (s, 1H), 8.32 (d, 7.2 Hz, 1H, NH); ^{13}C-NMR (150 MHz, DMSO-d_6): δ = 16.5, 17.3, 19.8, 32.8, 36.6, 45.6, 57.0, 61.7, 63.6, 66.4, 67.9, 69.8, 70.2, 71.8, 74.0, 76.3, 80.0, 81.3, 104.4, 105.6, 107.3, 108.1, 110.7, 114.7, 116.4, 116.8, 118.8,126.6, 127.8, 132.0, 135.2, 137.8, 138.1, 148.0, 152.0, 157.7, 165.0, 166.6, 167.3, 173.1, 185.6, 187.7; HRMS (ESI) : *m/z* = 884.3086 ($[M+H]^+$). Calcd. For $C_{42}H_{49}N_3O_{18}^+$ 884.3084.

Synthesis and Characterization of ***8***

To a solution of the crude PRM-A methyl ester (TFA salt, 20.8 mg, 21.5 μmol) in MeOH (8.0 mL) was added hydrazine monohydrate (52.0 μL, 1.08 mmol, 50 equiv.). The reaction mixture was stirred at room temperature for 7 hours, and then directly loaded onto Waters Sep-Pak® (Vac 35cc C_{18}-2g). After washing with H_2O containing 0.1% TFA, the gel was eluted with 50% MeCN/H_2O containing 0.1% TFA and the eluate was concentrated *in vacuo*. The residue was purified by reverse phase HPLC (system: Hitachi L-2130, column: YMC-Pack ODS-A, 5 μm, 20.0 mm ID x 250 mm; solvent: 40 min linear gradient 25–50% CH_3CN/H_2O containing 0.1% TFA; flow rate: 8.0 mL/min; UV: 254 nm; Rt: 20.3 min) to afford **8** (11.8 mg, 12.2 μmol, 57%; two-step yield from PRM-A) as a TFA salt.

$[\alpha]_D$: +207 (*c* = 0.203 in MeOH, 30 °C); ^{1}H-NMR (600 MHz, DMSO-d_6): δ = 1.30 (d, 6.6 Hz, 3H), 1.37 (d, 7.2 Hz, 3H), 2.33 (s, 3H), 2.70 (s, 3H), 3.12-3.21 (m, 3H), 3.34 (m, 1H), 3.45 (d,

3.0 Hz, 1H), 3.61 (s, br, 1H), 3.77 (dd, 4.8, 10.8 Hz, 1H), 3.92 (q, 6.6 Hz, 1H), 3.96 (s, 3H), 4.00 (dd, 3.6, 9.6 Hz, 1H), 4.52 (d, 6.6 Hz, 1H), 4.57 (q, 7.2 Hz, 1H), 4.61 (d, 9.0 Hz, 1H), 4.66 (d, 9.0 Hz, 1H), 4.77 (d, 7.2 Hz, 1H), 6.93 (d, 2.1 Hz 1H), 7.19 (s, 1H), 7.31 (d, 2.1 Hz, 1H), 8.07 (s, 1H), 8.56 (d, 6.0 Hz, 1H, NH); ^{13}C-NMR (150 MHz, DMSO-d_6): δ = 16.6, 17.7, 19.6, 36.6, 47.6, 57.0, 63.6, 66.3, 67.9, 69.8, 70.3, 71.7, 73.9, 76.2, 79.5, 81.2, 104.4, 105.3, 107.4, 108.3, 110.6, 114.6, 114.8, 116.3, 126.2, 128.0, 132.0, 134.9, 137.8, 138.3, 148.3, 151.4, 157.0, 165.0, 166.6, 167.7, 172.3, 185.5, 188.8; HRMS (ESI) : *m/z* = 877.2752 ([M+Na]$^+$). Calcd. For $C_{40}H_{46}N_4NaO_{17}^+$ 877.2750.

4.3. Sedimentation assay

To a solution of 1, 2.5, or 5 mM PRMs in distilled water (40 μL) in a 1.5 mL-Eppendorf tube was added 50 mM MOPS buffer (pH 7.0) containing 10 mM $CaCl_2$ (160 μL) at room temperature. The resulting mixture was incubated at 37 °C for 15 min and then at room temperature for 30 min. After centrifugation at 10,000 *g* for 5 min at 24 °C, the supernatant (30 μL) was poured into 50% CH_3CN aqueous solution containing 0.1% TFA (30 μL). The resulting solution was analyzed by reverse-phase HPLC (column: CAPCELL PAK C_{18} ACR, 5 μm, 4.6 mm ID × 250 mm; solvent: 25%–81% CH_3CN-water containing 0.1% TFA, 15-min linear gradient; flow rate: 1 mL/min; UV detection: 465 nm). The amount of non-precipitated PRMs was estimated from HPLC peak area and expressed as a percentage of the control.

4.4. ITC experiment

ITC measurements were carried out in 50 mM MOPS buffer (pH 7.0) containing 10 mM $CaCl_2$ at 30 °C using a Microcal iTC_{200} microcalorimeter (Microcal Inc., Northampton, MA). A typical titration consisted of injecting 1.0 μL of 200 mM solution of monosaccharide (total 40

injections) into 1 mM PRM with an interval of 2 min between injections at the stirrer speed of 1,000 rpm. The heat of dilution was determined under identical conditions by injecting the solution of Man-OMe into the ITC cell containing only the buffer. For every experiment, the heat of dilution was subtracted from the sample titration data before processing. The titration data were analyzed using the software provided by the manufacturer (Origin for ITC). The binding isotherm was fitted using a two-site binding model to calculate the dissociation constants (K_{d1} and K_{d2}).

4.5. Molecular modeling by DFT calculation

Initial structures of the [**4**$_2$/Ca^{2+}/(Man-OMe)$_2$], [**4a**$_2$/Ca^{2+}/(Man-OMe)$_2$], and [**4b**$_2$/Ca^{2+}/(Man-OMe)$_2$] complexes were built using the model structure of the [PRM-A$_2$/Ca^{2+}/(Man-OMe)$_2$] complex[18] by replacing PRM-A molecules with **4**, **4a**, and **4b**, respectively. The resulting initial structures were used for the geometry optimization at the theoretical level of ωB97X-D/6-31G(d). In each calculation, the most stable complex with Ca^{2+} was adopted among the calculated geometries. For interaction energies, BSSE (basis set superposition error) was taken into consideration. The Gaussian 16 program package[27] was used for all the DFT calculations. The calculations were carried out at the Center for Quantum Life Sciences (QuLiS) and at the Research Center for Computational Science, Okazaki National Research Institutes.

4.6. Antifungal assay

Candida rugosa AJ14513 was grown on the PDA plate (0.4% potato extract, 2.0% glucose, and 1.5% agar in water) at 30 °C for 24 h. The single colony (< 1 mm) was picked, and suspended in saline (1 mL) using platinum loop. The suspension (approximately 10^5 cfu/mL) was diluted 50 times with the RPMI medium (34.53 g/L MOPS in the RPMI1640, pH 7.0), and then further diluted 20 times. A total of 1,000 times diluted suspension (100 μL) was applied into each well

of a 96-well plate (Thermo Fisher Scientific). 2, 4, 8, 16, 32, 64, 128, and 258 μg/mL PRMs in RPMI medium containing 2.5% DMSO (100 μL) was added to each well. The resulting plate was allowed to incubate for 48 h at 35°C. The MIC values were determined by visual identification of fungal growth (n = 3).

Declaration of Competing Interest

The authors declare no conflict of interest.

Acknowledgements

This work was partly supported by JSPS KAKENHI Grant (Number 19K05712). We thank Mr. Kazushi Koga for assistance with the NMR spectroscopy analysis.

References

1. Oki T, Konishi M, Tomatsu K, Tomita K, Saitoh K, Tsunakawa M, Nishio M, Miyaki T, Kawaguchi H. Pradimicin, a novel class of potent antifungal antibiotics. *J. Antibiot.* 1988;41:1701–1704.
2. Takeuchi T, Hara T, Naganawa H, Okada M, Hamada M, Umezawa H, Gomi S, Sezaki M, Kondo S. New antifungal antibiotics, benanomicins A and B from an actinomycete. *J. Antibiot.* 1988;41:807–811.
3. Fukagawa Y, Ueki T, Numata K, Oki T. Pradimicins and benanomicins, sugar-recognizing antibiotics: Their novel mode of antifungal action and conceptual significance. *Actinomycetol*. 1993;7:1–22.
4. Oki T, Tenmyo O, Hirano M, Tomatsu K. Pradimicins A, B, and C: new antifungal antibiotics II. In vitro and in vivo biological activities. *J. Antibiot.* 1990;43:763–770.

5. Kakushima M, Masuyoshi S, Hirano M, Shinoda M, Ohta A, Kamei H, Oki T. In vitro and in vivo antifungal activities of BMY-28864, a water soluble pradimicin derivative. *Antimicrob. Agents Chemother.* 1991;35:2185–2190.
6. Sawada Y, Numata K, Murakami T, Tanimichi H, Yamamoto S, Oki T. Calcium-dependent anticandidal action of pradimicin A. *J. Antibiot.* 1990;43:715721.
7. Sawada Y, Murakami T, Ueki T, Fukagawa Y, Oki T, Nozawa Y. Mannan-mediated anticandidal activity of BMY-28864, a new water-soluble pradimicin derivative. *J. Antibiot.* 1991;44:119–121.
8. Tanabe A, Nakashima H, Yoshida O, Yamamoto N, Tenmyo O, Oki T. Inhibitory effect of new antibiotic, pradimicin A on infectivity cytopathic effect and replication of human immunodeficiency virus in vitro. *J. Antibiot.* 1988;41:1708–1710.
9. Balzarini J, Laethem KV, Daelemans D, Hatse S, Bugatti A, Rusnati M, Igarashi Y, Oki T, Schols D. Pradimicin A, a carbohydrate-binding nonpeptidic lead compound for treatment of infections with viruses with highly glycosylated envelopes, such as human immunodeficiency virus. *J. Virol.* 2007;81:362–373.
10. Alen MMF, Burghgraeve TD, Kaptein SJF, Balzarini J, Neyts J, Schols D. Broad antiviral activity of carbohydrate-binding agents against the four serotypes of dengue virus in monocyte-derived dendritic cells. *PLoS One* 2011;6:e21658.
11. Bertaux C, Daelemans D, Meertens L, Cormier EG, Reinus JF, Peumans WJ, Van Damme EJM, Igarashi Y, Oki T, Schols D, Dragic T, Balzarini J. Entry of hepatitis C virus and human immunodeficiency virus is selectively inhibited by carbohydrate-binding agents but not by polyanions. *Virology* 2007;366:40–50.
12. van der Meer FJUM, de Haan CAM, Schuurman NMP, Haijema BJ, Verheije MH, Bosch BJ, Balzarini J, Egberink HF. The carbohydrate-binding plant lectins and the non-peptidic

antibiotic pradimicin A target the glycans of the coronavirus envelope glycoproteins. *Antimicrob. Agents Chemother.* 2007;60:741–749.

13. Castillo-Acosta VM, Ruiz-Pérez LM, Etxebarria J, Reichardt NC, Navarro M, Igarashi Y, Liekens S, Balzarini J, González-Pacanowska D. Carbohydrate-binding non-peptidic pradimicins for the treatment of acute sleeping sickness in murine models. *PLoS Pathog.* 2016;12:e1005851.
14. Ueki T, Numata K, Sawada Y, Nishio M, Ohkura H, Kamachi H, Fukagawa Y, Oki T. Studies on the mode of antifungal action of pradimicin antibiotics II. D-Mannopyranoside-binding site and calcium-binding site. *J. Antibiot.* 1993;46:455–464.
15. Ueki T, Oka M, Fukagawa Y, Oki T. Studies on the mode of antifungal action of pradimicin antibiotics III. Spectrophotometric sequence analysis of the ternary complex formation of BMY-28864 with D-mannopyranoside and calcium. *J. Antibiot.* 1993;46:465–477.
16. Fujikawa K, Tsukamoto Y, Oki T, Lee YC. Spectroscopic studies on the interaction of pradimicin BMY-28864 with mannose derivatives. *Glycobiology* 1998;8:407–414.
17. Blaine J, Chonchol M, Levi M. Renal control of calcium, phosphate, and magnesium Homeostasis. *Clin. J. Am. Soc. Nephrol.* 2015;10:1257–1272.
18. Nakagawa Y, Doi T, Takegoshi K, Sugahara T, Akase D, Aida M, Tsuzuki K, Watanabe Y, Tomura T, Ojika M, Igarashi Y, Hashizume D, Ito Y. Molecular basis of mannose recognition by pradimicins and their application to microbial cell surface imaging. *Cell Chem. Biol.* 2019;26:950–959.
19. Nakagawa Y, Kakihara S, Tsuzuki K, Ojika M, Igarashi Y, Ito Y. A pradimicin-based staining dye for glycoprotein detection. *J. Nat. Prod.* 2021;84:2496–2501.
20. Nishio M, Ohkuma H, Kakushima M, Ohta S, Iimura S, Hirano M, Konishi M, Oki T. Synthesis and antifungal activities of pradimicin A derivatives modification of the alanine

moiety. *J. Antibiot.* 1993;46:494–499.

21. Kunishima M, Kawachi C, Iwasaki F, Terao K, Tani S. Synthesis and characterization of 4-(4,6-dimethoxy-1,3,5-triazin-2-yl)-4-methylmorpholinium chloride. *Tetrahedron Lett.* 1999;40:5327–5330.
22. Nakagawa Y, Doi T, Masuda Y, Takegoshi K, Igarashi Y, Ito Y. Mapping of the primary mannose binding site of pradimicin A. *J. Am. Chem. Soc.* 2011;133:17485–17493.
23. Bordwell FG, Fried HE, Hughes DL, Lynch TY, Satish AV, Whang YE. Acidities of carboxamides, hydroxamic acids, carbohydrazides, benzenesulfonamides, and benzenesulfonohydrazides in DMSO solution. *J. Org. Chem.* 1990;55:3330–3336.
24. Exner O, Simon W. Acyl derivatives of hydroxylamine. XII. Dissociation constants of hydroxamic acids and their functional derivatives. *Collect. Czech. Chem. Commun.* 1965;30:4078–4093.
25. Nakagawa Y, Yamaji F, Miyanishi W, Ojika M, Igarashi Y, Ito Y. Binding evaluation of pradimicins for oligomannose motifs from fungal mannans. *Bull. Chem. Soc. Jpn.* 2021;94:732–754.
26. Nakagawa Y, Doi T, Taketani T, Takegoshi K, Igarashi Y, Ito Y. Mannose-binding geometry of pradimicin A. *Chem. Eur. J.* 2013;19:10516–10525.
27. Gaussian 16, Revision C.01, Frisch MJ, Trucks GW, Schlegel HB, Scuseria GE, Robb MA, Cheeseman JR, Scalmani G, Barone V, Petersson GA, Nakatsuji H, Li X, Caricato M, Marenich AV, Bloino J, Janesko BG, Gomperts R, Mennucci B, Hratchian HP, Ortiz JV, Izmaylov AF, Sonnenberg JL, Williams-Young D, Ding F, Lipparini F, Egidi F, Goings J, Peng B, Petrone A, Henderson T, Ranasinghe D, Zakrzewski VG, Gao J, Rega N, Zheng G, Liang W, Hada M, Ehara M, Toyota K, Fukuda R, Hasegawa J, Ishida M, Nakajima T, Honda Y, Kitao O, Nakai H, Vreven T, Throssell K, Montgomery Jr. JA, Peralta JE, Ogliaro F,

Bearpark MJ, Heyd JJ, Brothers EN, Kudin KN, Staroverov VN, Keith TA, Kobayashi R, Normand J, Raghavachari K, Rendell AP, Burant JC, Iyengar SS, Tomasi J, Cossi M, Millam JM, Klene M, Adamo C, Cammi R, Ochterski JW, Martin RL, Morokuma K, Farkas O, Foresman JB, and Fox DJ, Gaussian, Inc., Wallingford CT, 2019.